Published in final edited form as:

Development. 2004 July ; 131(13): 3147–3156. doi:10.1242/dev.01187.

HUA ENHANCER3 reveals a role for a cyclin-dependent protein kinase in the specification of floral organ identity in *Arabidopsis*

Wenming Wang and **Xuemei Chen***

Waksman Institute, Rutgers University, 190 Frelinghuysen Road, Piscataway, NJ 08854, USA

Summary

In plants, organs are generated post-embryonically from highly organized structures known as meristems. Cell division in the meristem is closely integrated with cell fate specification and organ formation. The presence of multiple cyclin-dependent kinases (CDKs) and their partner cyclins in plants and other multicellular organisms probably reflects the complexity of cell cycle regulation within developmental contexts. The *Arabidopsis* genome encodes at least eight CDKs and 30 cyclins. However, no mutants in any CDKs have been reported, and the function of the great majority of these genes in plant development is unknown. We show that *HUA ENHANCER3* (*HEN3*), which encodes CDKE, a homolog of mammalian CDK8, is required for the specification of stamen and carpel identities and for the proper termination of stem cells in the floral meristem. Therefore, CDK8 plays a role in cell differentiation in a multicellular organism.

Keywords

Flower development; HEN3; Cyclin-dependent kinase

Introduction

The shoot apical meristem (SAM) serves as the ultimate source of the above-ground biomass in plants. Cells in the central zone of the SAM are stem cells that maintain the undifferentiated state, while cells in the peripheral zone participate in organ formation and eventually acquire various identities. Cell division in the meristem must be closely integrated with cell fate specification and organ formation. The SAM generates floral meristems after floral transition. A floral meristem, like the SAM, gives rise to lateral organs (sepals, petals and stamens), but unlike the SAM, terminates in a gynoecium. In *Arabidopsis*, the termination of stem cells in the floral meristem requires *AGAMOUS* (*AG*), a MADS-domain transcription factor (Bowman et al., 1989; Yanofsky et al., 1990). *AG* represses the expression of *WUSCHEL* (*WUS*), a stem cell maintenance gene, in a temporal manner in the floral meristem (Laux et al., 1996; Lenhard et al., 2001; Lohmann et al., 2001). *AG* also acts in floral organ identity specification. As a class C floral homeotic gene, *AG* specifies stamen identity together with the class B and *SEPALLATA* (*SEP*) genes and carpel identity

*Author for correspondence (xuemei@waksman.rutgers.edu).

Supplemental data available online

together with the *SEP* genes (Coen and Meyerowitz, 1991; Meyerowitz et al., 1991; Pelaz et al., 2000).

In addition to *AG*, several genes that act in the control of stamen and carpel identities and floral determinacy have been identified through sensitized genetic screens. Recessive mutations in *HUA1* and *HUA2, hua1-1* and *hua2-1*, respectively, were isolated as enhancers of the weak *ag-4* allele (Chen and Meyerowitz, 1999). *hua1-1 hua2-1* double mutant flowers show partial carpel-to-sepal and occasional stamen-to-petal transformation, phenotypes that are indicative of partial loss of class C activity (Chen et al., 2002; Chen and Meyerowitz, 1999; Western et al., 2002). In a genetic screen in the *hua1-1 hua2-1* background, recessive mutations in *HUA ENHANCER1* (*HEN1*), *HEN2, HEN4* and *PAUSED* (*PSD*), were found to enhance the weak floral homeotic phenotypes of *hua1-1 hua2-1* flowers such that stamens are transformed to petals and carpels are partially transformed to sepals (Chen et al., 2002; Cheng et al., 2003; Li and Chen, 2003; Western et al., 2002). The *HUA* and *HEN* genes all appear to directly or indirectly promote the expression of *AG* – in *hua1-1 hua2-1 hen* mutants, *AG* RNA or protein is of lower abundance than in wild type or in *hua1-1 hua2-1* (Cheng et al., 2003; Li and Chen, 2003). HUA1 and HEN4 physically interact in the nucleus, and together with HUA2 and HEN2 promote *AG* expression by preventing the production of alternative transcripts containing intron sequences (Cheng et al., 2003). *HEN1* is required for microRNA accumulation and may modulate *AG* expression or activity through regulation of *APETALA2*, a class A gene (Park et al., 2002; Chen, 2004)). In this study, we show that *HEN3*, which encodes an E-type CDK, also acts in the *AG* pathway.

CDKs are a family of serine/threonine protein kinases that control cell cycle progression, and/or coordinate cell cycle progression with transcription regulation. For a fully active state, they require both the association with regulatory subunits, cyclins and the phosphorylation of a conserved threonine residue by CDK-activating kinases (CAKs) (reviewed by Kobor and Greenblatt, 2002; Morgan, 1997). Among the nine known CDKs (CDK1–CDK9) in vertebrates, Cdc2 (CDK1) and CDK2 carry out central cell cycle functions (reviewed by Morgan, 1997). CDK4 and CDK6 are thought to integrate developmental signals and environmental cues into the cell cycle to drive cells through the G1-S transition. Cyclin D/CDK4 and cyclin D/CDK6 complexes phosphorylate the retinoblastoma protein (Rb), which renders Rb unable to associate with E2F and related transcription factors, thus allowing them to activate genes necessary for S-phase progression (reviewed by Harbour and Dean, 2000). Plants have both Rb-related (RBR) and E2F-related proteins (de Veylder et al., 2002; Huntley et al., 1998; Mariconti et al., 2002; Xie et al., 1996), but do not have orthologs of CDK4 or CDK6 (Dewitte and Murray, 2003; Vandepoele et al., 2002). Three CDKs, CDK7, CDK8 and CDK9, function in transcriptional regulation. CDK7 is in the TFIIH complex, where it phosphorylates the C-terminal domain (CTD) of the largest subunit of RNA polymerase II to promote transcription elongation (Kobor and Greenblatt, 2002). CDK9/cylin T belongs to the positive transcription elongation factor b (P-TEFb) complex, which phosphorylates the CTD to promote transcription elongation (de Falco and Giordano, 2002).

In mammalian cells, CDK8/cyclin C is a component of RNA polymerase II holoenzyme and serves as a repressor of transcription through two mechanisms. It phosphorylates the cyclin

H subunit of TFIIH and this leads to the repression of the ability of TFIIH to activate transcription and the inhibition of the CTD kinase activity of CDK7 (Akoulitchev et al., 2000). It also phosphorylates the CTD of RNA polymerase II prior to the formation of the preinitiation complex to result in inhibition of transcription (Liao et al., 1995; Rickert et al., 1996; Sun et al., 1998). Although the developmental functions of CDK8 in higher eukaryotes are currently unknown, CDK8 proteins from yeast and *Dictyostelium* appear to act in cell differentiation in response to nutrient conditions. Srb10p, the yeast CDK8, regulates filamentous growth in response to nutrient limitation (Nelson et al., 2003). The *Dictyostelium* CDK8 is required for aggregation, which leads to sporulation, under starvation (Takeda et al., 2002).

The *Arabidopsis* genome encodes eight CDKs classified into the A, B, C and E types, and 30 cyclins classified into the A, B, D and H types, according to sequence similarity among themselves and with their mammalian counterparts (Vandepoele et al., 2002). Of the four types of CDKs, A and B types have been best studied in plants. A-type CDKs regulate both the G1-S and G2-M transitions, whereas B-type CDKs control the G2-M transition (Hemerly et al., 1995; Magyar et al., 1997; Porceddu et al., 2001). CDKAs have the PSTAIRE cyclin binding motif and are associated with D-type cyclins (Dewitte and Murray, 2003; Vandepoele et al., 2002). Two CDKCs in *Arabidopsis* share a PITAIRE cyclin-binding signature and other structural characteristics with mammalian CDK9. They interact with proteins sharing homology with the cyclin partners of CDK9, cyclin T and cyclin K (Barroco et al., 2003). An E-type CDK with a SPTAIRE cyclin-binding motif was first found in alfalfa (Magyar et al., 1997), and later a related sequence was identified in *Arabidopsis* (Vandepoele et al., 2002). The function of CDKE is unknown.

Here we show that HEN3 encodes the only *Arabidopsis* E-type CDK. We also show that HEN3 shares significant sequence similarity to CDK8 and, like CDK8, HEN3 exhibits CTD kinase activity. Phenotypic characterization of *hen3* mutants demonstrates that HEN3 acts in cell expansion in leaves and cell fate specification in floral meristems. Our studies demonstrate a role of CDK8 in cell differentiation in a multicellular organism.

Materials and methods

Isolation of *hen3* mutations

hua1-1 hua2-1 seeds were mutagenized as described (Chen et al., 2002). Single M2 families were screened and three independent lines with *ag*-like floral phenotypes were identified. The mutations were recovered from the fertile siblings. Complementation tests with plants heterozygous for each mutation showed that the three alleles are in the same gene, which we named *HEN3*. The three *hen3* lines were backcrossed to *hua1-1 hua2-1* three times to clean up the genetic background. The *hua1-1 hua2-1 hen3* triple mutants were then crossed to either *hua1-1* or *hua2-1* to obtain *hua1-1 hen3* or *hua2-1 hen3* double mutants. The two double mutants were then crossed to each other to obtain *hen3* single mutants. In these crosses, molecular genotyping for *hua1-1* and *hua2-1* (Chen and Meyerowitz, 1999; Li et al., 2001) facilitated the identification of plants of the expected genotypes.

Map-based cloning of *HEN3*

hua1-1 hua2-1 hen3-1/+ plants (in the Landsberg ecotype) were crossed to *hua1-1 hua2-1*(Col), a line in which the *hua1-1* and *hua2-1* mutations were introgressed into the Columbia background. Five hundred and two plants with the *hua1-1 hua2-1 hen3-1* phenotypes in the F2 population were used for mapping. *HEN3* was initially mapped close to *HEN4* on chromosome V with the markers used to isolate *HEN4* (Cheng et al., 2003). New markers were developed based on the Cereon Genomics SNPs and used to map *HEN3* to a region of ~150 kb covered by P1 clones MBK5, MGI19, MLE2 and MBM17 (see Figure S1A at http://dev.biologists.org/supplemental). We sequenced 12 candidate genes in this region from *hua1-1 hua2-1 hen3-1* plants and found a C-to-T mutation that would result in a stop codon in At5g63610. Sequencing of At5g63610 from *hen3-2* and *hen3-3* plants uncovered separate G-to-A mutations that would result in R-to-K and G-to-R amino acid substitutions, respectively (Fig. 4B). A fragment covering At5g63610 was amplified by PCR with primers MBK5p7 (5′tggttccgttggagaaattgacataaa 3′) and MBK5p8 (5′gttggtggtaaatagataagactggcagg 3′) (see Fig. S1A at http://dev.biologists.org/supplemental), and cloned into pPZP211 (Hajdukiewicz et al., 1994). The resulting plasmid, pHEN3g, was transformed into *hen3-1* and *hua1-1 hen3-1* plants and found to rescue the silique length defects of these plants (see Fig. S1B at http://dev.biologists.org/supplemental). To determine whether the clone also rescues the *hua1-1 hua2-1 hen3-1* floral homeotic phenotypes, a *hua1-1 hen3-1* plant hemizygous for the HEN3g transgene was crossed to *hua2-1 hen3-1*. F2 seeds were plated on Kanamycin medium to select for the HEN3g transgene and Kanamycin resistant F2 plants were transferred to soil and screened to identify those with floral phenotypes that resembled *hua1-1 hua2-1*. Three such plants were obtained from a total of 56 F2 plants. The three plants were then genotyped for *hua1-1* and *hua2-1* and confirmed to be homozygous for both mutations. Therefore, these plants were *hua1-1 hua2-1 hen3-1* triple mutants that carried the HEN3g transgene. As they exhibited *hua1-1 hua2-1*-like floral phenotypes, the transgene rescued the floral homeotic phenotypes conferred by the *hen3-1* mutation.

HEN3 plasmid construction

The 5′ and 3′ ends of *HEN3* RNA were determined by 5′ and 3′ RACE, respectively. The GenBank Accession Number for *HEN3* cDNA is AY600243.

To generate a HEN3-GUS reporter construct, a GUS-NOS cassette was released from pBI121 by *Eco*RI/*Bam*HI and cloned into pPZP211 to generate pPZP211-GUS. The *HEN3*-coding region plus 1.5 kb of sequences upstream of the start codon was amplified with primers MBK5p7 and MBK5P10 (5′gaggcgtctggatttgttaggaggt 3′) and cloned into pPZP211-GUS. The resulting plasmid pPZP211-HEN3-GUS was transformed into L*er* and *hen3-1* plants. The construct largely rescued the *hen3-1* vegetative defects. The L*er* transformants were used to determine the expression profiles of *HEN3* by GUS staining.

The *HEN3*-coding region plus 1.5 kb of sequences upstream of the start codon was cloned into pPZP211-HA to provide an HA tag to the C terminus of HEN3. The resulting plasmid pPZP211-HEN3-HA was transformed into *hen3-1* plants and found to largely rescue the

silique defects of *hen3-1* (Fig. S1B at http://dev.biologists.org/supplemental). These *hen3-1 HEN3-HA* plants were used to immunoprecipitate HEN3-HA in the protein kinase assay.

RNA filter hybridization and scanning electron microscopy (SEM)

RNA filter hybridization was carried out as described (Li et al., 2001). Total RNA (40 μg) was used to detect *AG* and *AP1* RNAs. PolyA$^+$ RNA (1 μg) was used to detect *HEN3* RNA. Hybridization signals were quantified with a phosphorimager.

SEM was carried out as described previously (Chen et al., 2002).

Protein expression in *E. coli*

The C-terminal domain (CTD) of the largest subunit of RNA polymerase II from *Arabidopsis* (Dietrich et al., 1990) was amplified by RT-PCR using primers CTDp1 (5′-CCTGGATCCAGTCCTACTTCTCCCGGTTACAGT-3′) and CTDp2 (5′-CCTGGATCCTGGATTGCCAATTCTCACTCTCTT-3′). The amplified CTD fragment was cloned into the *E. coli* expression vector pRSETA to generate pRSETA-CTD. The His-tagged CTD polypeptide was expressed in the *E. coli* strain BL21DE3pLysS and purified according to manufacturer's instruction (Qiagen).

Histone H1 was purchased from Roche (CAT#0223549). His-GFP was produced with the Rapid Translation System from Roche (CAT#3186148).

Kinase assay

Kinase assay was carried out according to the method reported by Cockcroft et al. (Cockcroft et al., 2000). Briefly, 10 g of inflorescences was ground in liquid nitrogen and suspended in 50 ml of extraction buffer [50 mM Tris-HCl (pH 7.5), 75 mM NaCl, 15 mM EGTA, 15 mM $MgCl_2$, 1 mM NaF, 0.2 mM sodium orthovanadate, 2 mM Na-pyrophosphate, 60 mM glycerol 2-phosphate, 1 mM DTT, 0.1% Tween 20, 1×protease inhibitor mix (Roche, #1697498)]. The suspension was filtered through one layer of cheesecloth and two layers of miracloth and centrifuged at 1900 ***g*** for 20 minutes at 4°C. The supernatant was transferred to a new tube and centrifuged again. Finally, 40 ml of supernatant was added to 160 μl of 50% anti-HA (or anti-protein C as a control)-coupled matrix slurry and incubated with gentle rotation at 4°C for 1 hour. The beads were precipitated by centrifugation at 120 ***g*** for 10 minutes, washed three times with wash buffer (50 mM Tris-HCl pH 7.5, 250 mM NaCl, 5 mM EDTA, 5 mM NaF, 0.1% Tween 20, 0.5 mM PMSF), two times with kinase buffer (50 mM Tris-HCl pH 7.5, 100 mM NaCl, 15 mM EGTA, 1 mM DTT) and resuspended in 20 μl of assay buffer (50 mM Tris-HCl pH 7.5, 100 mM NaCl, 10 mM $MgCl_2$, 10 mM $MnCl_2$, 1 mM DTT, 0.5 mM PMSF, 0.5 μg/μl purified His-CTD, 2 μCi [γ-^{32}P]ATP). The reaction mixture was incubated at room temperature for 25 minutes. His-GFP protein was used as a negative control, while histone H1 was used as a potential alternative substrate. The reaction was stopped by adding SDS-PAGE loading buffer and boiling for 5 minutes. Samples were analyzed by SDS-PAGE.

Results

HEN3 is required for cell fate specification in flowers

We performed a genetic mutagenesis screen in the *hua1-1 hua2-1* background to search for genes acting in floral meristems to control stem cell termination and lateral organ identities. We isolated three recessive mutations in a gene we named *HUA ENHANCER3* (*HEN3*). *hen3-1, hen3-2*, and *hen3-3* all resulted in loss of reproductive organ identity and floral determinacy in the *hua1-1 hua2-1* background. While the third whorl organs were stamens in wild-type and *hua1-1 hua2-1* flowers, petals were the predominant type of organs in the third whorl of *hua1-1 hua2-1 hen3* flowers (Table 1, Fig. 1A–D). Although stigmatic tissue was found on some fourth whorl organs in *hua1-1 hua2-1 hen3-1* and *hua1-1 hua2-1 hen3-2* flowers (Fig. 1C,D), all abaxial epidermal cells on these organs showed epicuticular striations similar to those on abaxial sepal cells (Fig. 1H). By contrast, the majority of epidermal valve cells on *hua1-1 hua2-1* ovaries exhibited a smooth surface characteristic of normal ovary valve cells (Fig. 1G). The number of fourth whorl organs in *hua1-1 hua2-1 hen3-1* and *hua1-1 hua2-1 hen3-2* flowers was increased (Table 1). In addition, internal flowers were present in all *hua1-1 hua2-1 hen3* flowers (Fig. 1E and data not shown). These phenotypes suggest that *HEN3* acts in the specification of stamen and carpel identities and floral determinacy in *Arabidopsis* flower development. The *hen3-2* allele is the most severe among the three in the floral phenotypes – staminoid petals were found in the third whorl of *hua1-1 hua2-1 hen3-1* or *hua1-1 hua2-1 hen3-3* but not *hua1-1 hua2-1 hen3-2* flowers (Table 1). No organ identity or floral determinacy defects were obvious in *hua1-1 hen3, hua2-1 hen3* or *hen3* mutants (Fig. 1F; data not shown). However, all *hua1-1 hen3, hua2-1 hen3* double mutants and *hen3* single mutants produced shorter siliques and stems than the corresponding *HEN3* genotypes (Fig. S1 and data not shown).

Consistent with the floral phenotypes, we found that *hua1-1 hua2-1 hen3-1* flowers were defective in the spatial control of *AP1* expression and the temporal control of *WUS* expression in flower development. *AP1* RNA is found throughout the floral primordium during stages 1–2 but is restricted to the outer two floral whorls starting at stage 3 because of repression of its expression by *AG* in the inner two whorls (Gustafson-Brown et al., 1994; Mandel et al., 1992). At stage 3, *AP1* RNA accumulation patterns in *hua1-1 hua2-1* flowers were similar to those in wild type (Chen and Meyerowitz, 1999) (Fig. 2A). However, in *hua1-1 hua2-1 hen3-1* stage 3 flowers, as in *ag-3* flowers, *AP1* RNA was found throughout the floral primordium (Fig. 2B). The ectopic expression of *AP1* in the inner two floral whorls was found in *hua1-1 hua2-1 hen3-1* flowers of all stages (data not shown). *WUS* is expressed in a few cells underneath the presumed stem cells in the floral meristem till stage 6, when *AG* acts to terminate its expression (Mayer et al., 1998). Although *WUS* RNA was not observed in stage 7 and older *hua1-1 hua2-1* flowers (Fig. 2C), *WUS* RNA was readily detected in stage 7 and older *hua1-1 hua2-1 hen3-1* (Fig. 2D) and *hua1-1 hua2-1 hen3-2* (data not shown) flowers.

HEN3 acts primarily in the *AG* pathway in flower development

As *HEN3* acts similarly to *AG* in flower development, we asked whether *HEN3* acts in the *AG* pathway or in a parallel pathway. If *HEN3* acts strictly in the *AG* pathway, we would

expect *hua1-1 hua2-1 hen3-1 ag-1* flowers to be identical to *ag-1* flowers in all phenotypes. Indeed, *ag-1* was essentially epistatic to *hua1-1 hua2-1 hen3-1* in that only perianth organs were present in *hua1-1 hua2-1 hen3-1 ag-1* flowers (Fig. 1I). However, there appeared to be more whorls of petals than those of sepals in the quadruple mutant flowers. To investigate this further, we constructed the *hen3-1 ag-1* double mutant and found that *hen3-1* caused partial sepal-to-petal transformation in the fourth whorl of *ag-1* flowers (Fig. 1J). This was probably the reason for the presence of more petals in the quadruple mutant. Therefore, *HEN3* has functions overlapping with, but not identical to, those of *AG* in organ identity specification. In terms of floral determinacy, *HEN3*, as well as *HUA1* and *HUA2*, appeared to act in the *AG* pathway as *hen3-1* did not enhance *ag-1* in this phenotype. *AG* and *CLV1* both control floral determinacy by regulating the expression of *WUS*. However, the molecular mechanisms differ – while *AG* represses *WUS* in a temporal manner, *CLV1* restricts the domain of *WUS* expression (Schoof et al., 2000). In fact, *ag-1* enhances *clv1-1* in floral determinacy defects (Clark et al., 1993). If *HUA1, HUA2* and *HEN3* act in the *AG* pathway in floral determinacy, we would expect *hua1-1, hua2-1* and *hen3-1* to enhance the severe *clv1-4* allele in floral determinacy defects. Indeed, *hua1-1 hua2-1 hen3-1 clv1-4* flowers showed dramatic enlargement of the floral meristem, such that a massive group of apparently undifferentiated cells accumulated in the center of the flower (Fig. 1L). This dramatic phenotype was not observed in either *hua1-1 hua2-1 hen3-1* or *clv1-4* (Fig. 1K) flowers.

Mutations in *HEN1, HEN2, HEN4* and *PSD* all resulted in reduced *AG* expression in the *hua1-1 hua2-1* background (Cheng et al., 2003; Li and Chen, 2003), which was consistent with the floral homeotic phenotypes caused by these mutations. The *hen3* mutations lead to more severe loss-of-C-function phenotypes when compared with the other *hen* mutations. We performed RNA filter hybridization to determine whether the *hen3-1* mutation also results in reduced *AG* RNA levels in the *hua1-1 hua2-1* background. Three *AG* RNAs, RNA1, RNA2 and *AG* mRNA, can be detected in *hua1-1 hua2-1* and *hua1-1 hua2-1 hen3-1* flowers (Fig. 3A). RNA1 and RNA2 are second intron-containing *AG* RNAs that cannot generate the full-length AG protein (Cheng et al., 2003). Although mutations in *HEN2, HEN4, HUA1* and *HUA2* lead to increased abundance of RNA1 and RNA2, and a concomitant decrease in abundance of *AG* mRNA (Cheng et al., 2003), *hen3-1* resulted in an increase in abundance in both the intron-containing RNAs and the mRNA in the *hua1-1 hua2-1* background (Fig. 3A). The abundance of *AP1* (Fig. 3A) and *AP2* (not shown) was also increased in *hua1-1 hua2-1 hen3-1* flowers relative to *hua1-1 hua2-1* flowers.

In situ hybridization showed that the timing and domain of *AG* mRNA accumulation in *hua1-1 hua2-1 hen3-1* flowers were normal (data not shown). AG protein abundance was similar between *hua1-1 hua2-1* and *hua1-1 hua2-1 hen3-1* flowers (Fig. 3B).

HEN3 encodes CDKE

To begin to understand the molecular functions of *HEN3*, we cloned this gene with a map-based approach (see Materials and methods; Fig. S1). The predicted HEN3 (At5g63610) protein shares significant sequence similarity to plant and animal cyclin-dependent protein kinases (Fig. 4A,B), and was classified as an E-type CDK with a SPTAIRE cyclin binding

motif in the kinase domain (Joubes et al., 2000; Vandepoele et al., 2002). HEN3 and related proteins from alfalfa and rice are currently the only members of the E class of plant CDKs (Fig. 4C), for which no cellular or developmental functions are known. Class E CDKs appear to be more related to CDK8 throughout the kinase domain than any other CDKs in metazoans (Fig. 4C). In vertebrates, CDK8, in association with cyclin C, phosphorylates the CTD of the largest subunit of RNA polymerase II (Liao et al., 1995; Rickert et al., 1996). Interestingly, HEN3 contains a SPTAIRE cyclin binding motif that differs from the SMSACRE motif from CDK8 but resembles the PSTAIRE motif from plant CDKAs (Fig. 4B). Plant CDKAs are more closely related to human CDK1 (cdc2), CDK2 and CDK3 than to CDK8 (Fig. 4C).

To test whether HEN3 possesses protein kinase activity, we generated transgenic lines in which HEN3 was tagged with the HA epitope in a translational fusion under the control of the *HEN3* promoter. The *HEN3-HA* transgene was able to rescue the *hen3-1* silique (Fig. S1B at http://dev.biologists.org/supplemental) and stem elongation defect (not shown), suggesting that the fusion protein was functional. We then immunoprecipitated HEN3-HA from these plants using an anti-HA monoclonal antibody and performed a kinase assay using *E. coli* produced, 6×His-tagged *Arabidopsis* CTD, 6×His-GFP and human Histone H1 as substrates. Anti-HA, but not the control anti-protein C immunoprecipitate, was able to phosphorylate 6×His-CTD, but not 6×His-GFP or human Histone H1 (Fig. 5A). Anti-HA immunoprecipitates from non-transformed plants did not result in CTD phosphorylation (Fig. 5B). It has previously been shown that the *Arabidopsis* CDKA/cyclin D complex and a tobacco CDK2a/cyclin D3 complex were able to phosphorylate the maize RBR in vitro (Boniotti and Gutierrez, 2001; Nakagami et al., 1999). The HEN3-HA immunoprecipitate was unable to phosphorylate the maize RBR (not shown). Therefore, CDKE has distinct substrate specificity from that of CDKA. It should be noted that the *hen3-1* mutation deletes part of the kinase domain and the *hen3-2* and *hen3-3* mutations are in amino acids that are conserved among many CDKs (Fig. 4B and data not shown). Therefore, it is likely that the kinase activity of HEN3 is compromised or abolished in these mutants.

HEN3 is expressed in proliferating tissue

CDKs involved in cell cycle progression are preferentially expressed in dividing tissues (Dewitte and Murray, 2003). To determine if HEN3 is expressed preferentially in proliferating tissue, we generated a translational fusion of HEN3 to β-glucuronidase (GUS) under the control of the *HEN3* promoter. This fusion construct was introduced into *hen3-1* and found to largely rescue the *hen3-1* vegetative phenotypes. Histochemical staining for GUS activity showed that *HEN3* is expressed in young, presumably dividing, tissue, such as shoot and root tips, lateral root primordia, young leaves, and flowers (Fig. 2E–H). We performed in situ hybridization to determine the localization of *HEN3* RNA in inflorescence meristems and in flowers. *HEN3* RNA was present throughout the inflorescence meristem, the inflorescence stem and young flowers (Fig. 2I,J). The uniform presence of *HEN3* RNA in every cell in inflorescence and floral meristems indicates that *HEN3* RNA abundance is not regulated in a cell cycle dependent manner. The alfalfa CDKE gene is also expressed at a basal unchanged level throughout the cell cycle (Magyar et al., 1997).

RNA filter hybridization showed that *HEN3* RNA was present in leaves, stems, roots (not shown) and inflorescences (Fig. 3C). *HEN3* RNA was more abundant in *ag-3* inflorescences (Fig. 3C). This may suggest that *HEN3* is negatively regulated by *AG*. However, the increased *HEN3* RNA abundance in *ag-3* inflorescences may simply be due to a higher amount of proliferating tissue in *ag-3* flowers.

HEN3 is required for cell expansion in leaves

We observed that all three *hen3* alleles resulted in the reduction of leaf size (Fig. 6A–C). This and the fact that HEN3 encodes a CDK raised the question of whether HEN3 plays a direct role in cell division. Therefore, we sought to determine whether the reduction in leaf size in *hen3* mutants was due to reduced cell number or cell size. We measured the area of the fully expanded fifth leaf in wild-type and the three *hen3* mutants. The most severe *hen3-2* allele caused a nearly 50% reduction in leaf size (Fig. 6D). We next performed scanning electron microscopy to examine leaf adaxial epidermal cells in the four genotypes. Although leaf epidermal cells from the same leaf can vary greatly in cell size in all genotypes (hence the large standard error), the *hen3* mutants had, on average, smaller cells than wild type (Fig. 6E). In the same unit area in a leaf, the *hen3* mutants had more epidermal cells (Fig. 6F). Taking into account the differences in leaf size, these genotypes have roughly the same number of cells in the fifth leaves. Therefore, it appears that the reduction in leaf size caused by *hen3* mutations is due to reduced cell expansion rather than cell division. Consistent with this, we did not observe any differences in the morphology of the SAM or leaf primordia between L*er* and *hen3-1* in longitudinal sections or by SEM (Fig. S2 at http://dev.biologists.org/supplemental). In situ hybridization showed that histone H4, a gene known to be expressed in a cell cycle-dependent manner, was expressed similarly in wild-type and *hen3-1* SAMs, and leaf primordia (see Fig. S2 at http://dev.biologists.org/supplemental).

hen3 single mutant plants also exhibited shorter stems and siliques (see Fig. S1B at http://dev.biologists.org/supplemental). The valve cells of *hen3* siliques were shorter than those in wild type (data not shown). Root growth on media with or without sucrose was similar in wild-type and *hen3-1* plants (see Fig. S3 at http://dev.biologists.org/supplemental; data not shown).

Discussion

HEN3 and CDK8

Phylogenetically, HEN3 groups with CDK8 proteins from yeast, *Dictyostelium* and metazoans. In mammals and yeast, CDK8 forms a complex with cyclin C and phosphorylates the CTD of the largest subunit of RNA polymerase II (Kobor and Greenblatt, 2002). The phosphorylation status of the CTD is dynamically controlled by kinases and phosphatases during transcription initiation and elongation and appears to dictate different roles the CTD plays during transcription, which include inhibition or promotion of transcription and recruitment of various RNA processing proteins to sites of transcription (Oelgeschlager, 2002). In mammals and yeast, CDK8/cyclinC is part of a complex that interacts specifically with RNA polymerase II and represses activated transcription, i.e.

transcription activated by specific transcription factors (Akoulitchev et al., 2000; Sun et al., 1998). HEN3 possesses, or is associated with, a kinase activity that phosphorylates the *Arabidopsis* CTD. Therefore, it is possible that HEN3, like CDK8, plays a regulatory role in transcription. Consistent with a negative regulatory role of HEN3 in transcription, the abundance of *AG, AP1* and *AP2* RNAs is elevated by the *hen3-1* mutation in the *hua1-1 hua2-1* background. It is not known how general the effect of the *hen3* mutations on transcription is. However, clearly all genes are not affected to the same extent as the elevation of *AG, AP1* and *AP2* RNA abundance was seen relative to *UBQ5* RNA abundance. It is also possible that the increased abundance of *AG, AP1*, and *AP2* RNAs is due to genetic interaction between *hen3-1* and the *hua* mutations.

The cyclin partner of HEN3, a CDK8 homolog in plants, remains to be determined. Intriguingly, HEN3 contains a cyclin-binding motif that is very similar to that of CDKA, which interacts with D-type cyclins that are thought to integrate inputs from developmental and environmental signals into the cell cycle (Meijer and Murray, 2000; Riou-Khamlichi et al., 1999). Therefore, it may be predicted that HEN3 partners with D-type cyclins, although CDK8 partners with cyclin C. No C-type cyclins from *Arabidopsis* have been described, but the genome appears to contain at least two C-type cyclins (At5g48630 and At5g48640). In addition, a rice C-type cyclin has been reported (Yamaguchi et al., 2000). At5g48640 did not interact with HEN3 in a yeast two-hybrid assay (W. Wang and X. Chen, unpublished). By contrast, a yeast two-hybrid screen using HEN3 as the bait resulted in the isolation of three D-type cyclins that can interact with HEN3 in yeast (W.W. and X.C., unpublished).

Developmental roles of *HEN3*

HEN3 RNA and protein (HEN3-GUS) are present in proliferating tissue, where cells need to coordinate developmental events such as cell division, expansion and fate specification. *HEN3* seems to be required for cell expansion in leaves and cell fate specification in floral meristems. Although a direct role of *HEN3* in cell division is not obvious from the *hen3* mutant phenotypes, its mammalian homolog CDK8 controls cell proliferation through negative regulation of TFIIH transcription activity (Akoulitchev et al., 2000). We speculate that *HEN3* can be a potential link between cell division and cell fate specification in the floral meristem. For example, key regulators of cell division and cell fate specification may be coordinately regulated by *HEN3* through either transcriptional regulation or phosphorylation, thus linking cell division control to cell fate specification. Alternatively, *HEN3* activity may be regulated by the cell cycle, which ensures that the function of *HEN3* in cell fate specification is integrated with cell division. Although *HEN3* RNA or HEN3-GUS does not accumulate in a cell cycle-dependent manner, HEN3 activity may be regulated by the cell cycle through its partner cyclins.

How might *HEN3* be involved in cell expansion? Plant cell expansion can be influenced by many processes, such as cell wall relaxation or reorganization, endoreduplication, cytoskeleton remodeling and hormone signaling (reviewed by Clouse and Sasse, 1998; Cosgrove, 1993; Sugimoto-Shirasu and Roberts, 2003; Wasteneys and Galway, 2003). *HEN3* may directly or indirectly affect the expression or function of genes in any of these processes.

How *HEN3* acts in the *AG* pathway is currently unknown. Our previous work showed that *HUA1, HUA2, HEN2*, and *HEN4* prevent transcription termination within the second intron of *AG*. Mutations in these genes result in reduced abundance of *AG* mRNA and increased abundance of *AG* RNA1 and RNA2, transcripts that terminate in the second intron. HEN3 is able to phosphorylate the CTD, which regulates transcription elongation and coordinates RNA processing with transcription elongation. Therefore, it is plausible that HEN3 is also involved in alternative transcript production from *AG*. However, the *hen3-1* mutation leads to increased accumulation of not only *AG* RNA1 and RNA2 but also *AG* mRNA. This can be best explained by a role of HEN3 in repressing transcription, as has been demonstrated for mammalian and yeast CDK8 proteins. One possible explanation for the loss of C-function phenotypes caused by *hen3* mutations is that the *hen3* mutations lead to higher levels of RNAs from class A genes than from *AG*, such that A function wins over C function during flower development. Alternatively, HEN3 may play an indirect role in organ identity through its primary function in cell division or cell elongation. It is conceivable that missing cells or altered timing of cell elongation in organ primordia may influence their identities. However, we have not observed gross differences in developing organ primordia between wild-type and *hen3* mutants. Finally, *HEN3* may regulate class A or C proteins by phosphorylation. A recent study showed that the budding yeast cdc28 kinase, a key cell cycle regulator, phosphorylates not only proteins that drive cell cycle events but also other regulatory proteins to supposedly orchestrate global gene expression throughout the cell cycle (Ubersax et al., 2003). Another study demonstrated that Srb10, the budding yeast homolog of CDK8, regulates yeast filamentous growth in response to nutrient conditions by phosphorylating, and thus regulating, Ste12, a transcription factor required for filamentous growth (Nelson et al., 2003). It is possible that HEN3 acts as a class C gene by phosphorylating either class C or class A proteins.

Supplementary Material

Refer to Web version on PubMed Central for supplementary material.

Acknowledgments

We thank Drs Benedicte Desvoyes and Crisanto Gutierrez for the maize RBR plasmid, Dr Guozheng Liu for suggestions on protein kinase assays, and Dongxuan Jia for her help during the map-based cloning of *HEN3*. We thank Randy Kerstetter, Yael Harrar and Junjie Li for helpful comments on the manuscript. This work was supported by an NIH grant (GM61146) to X.C.

References

Akoulitchev S, Chuikov S, Reinberg D. TFIIH is negatively regulated by cdk8-containing mediator complexes. Nature. 2000; 407:102–106. [PubMed: 10993082]

Barroco RM, de Veylder L, Magyar Z, Engler G, Inze D, Mironov V. Novel complexes of cyclin-dependent kinases and a cyclin-like protein from *Arabidopsis* thaliana with a function unrelated to cell division. Cell. Mol. Life Sci. 2003; 60:401–412. [PubMed: 12678503]

Boniotti MB, Gutierrez C. A cell-cycle-regulated kinase activity phosphorylates plant retinoblastoma protein and contains, in *Arabidopsis*, a CDKA/cyclin D complex. Plant J. 2001; 28:341–350. [PubMed: 11722776]

Bowman JL, Smyth DR, Meyerowitz EM. Genes directing flower development in *Arabidopsis*. Plant Cell. 1989; 1:37–52. [PubMed: 2535466]

Chen X. A microRNA as a translational repressor of *APETALA2* in Arabidopsis flower development. Science. 2004; 303:2022–2025. [PubMed: 12893888]

Chen X, Meyerowitz EM. *HUA1* and *HUA2* are two members of the floral homeotic *AGAMOUS* pathway. Mol. Cell. 1999; 3:349–360. [PubMed: 10198637]

Chen X, Liu J, Cheng Y, Jia D. *HEN1* functions pleiotropically in *Arabidopsis* development and acts in C function in the flower. Development. 2002; 129:1085–1094. [PubMed: 11874905]

Cheng Y, Kato N, Wang W, Li J, Chen X. Two RNA binding proteins, HEN4 and HUA1, act in the processing of *AGAMOUS* pre-mRNA in *Arabidopsis thaliana*. Dev. Cell. 2003; 4:53–66. [PubMed: 12530963]

Clark SE, Running MP, Meyerowitz EM. *CLAVATA1*, a regulator of meristem and flower development in *Arabidopsis*. Development. 1993; 119:397–418. [PubMed: 8287795]

Clouse SD, Sasse JM. Brassinosteroids: essential regulators of plant growth and development. Annu. Rev. Plant Physiol. Plant Mol. Biol. 1998; 49:427–451. [PubMed: 15012241]

Cockcroft CE, den Boer BG, Healy JM, Murray JA. Cyclin D control of growth rate in plants. Nature. 2000; 405:575–579. [PubMed: 10850717]

Coen ES, Meyerowitz EM. The war of the whorls: genetic interactions controlling flower development. Nature. 1991; 353:31–37. [PubMed: 1715520]

Cosgrove DJ. Wall extensibility: its nature, measurement and relationship to plant cell growth. New Phytol. 1993; 124:1–23. [PubMed: 11537718]

de Falco G, Giordano A. CDK9: from basal transcription to cancer and AIDS. Cancer Biol. Ther. 2002; 1:342–347. [PubMed: 12432243]

de Veylder L, Beeckman T, Beemster GT, de Almeida Engler J, Ormenese S, Maes S, Naudts M, van Der Schueren E, Jacqmard A, Engler G, et al. Control of proliferation, endoreduplication and differentiation by the *Arabidopsis* E2Fa-DPa transcription factor. EMBO J. 2002; 21:1360–1368. [PubMed: 11889041]

Dewitte W, Murray JA. The plant cell cycle. Annu. Rev. Plant Biol. 2003; 54:235–264. [PubMed: 14502991]

Dietrich MA, Prenger JP, Guilfoyle TJ. Analysis of the genes encoding the largest subunit of RNA polymerase II in *Arabidopsis* and soybean. Plant Mol. Biol. 1990; 15:207–223. [PubMed: 2103447]

Gustafson-Brown C, Savidge B, Yanofsky MF. Regulation of the *Arabidopsis* floral homeotic gene *APETALA1*. Cell. 1994; 76:131–143. [PubMed: 7506995]

Hajdukiewicz P, Svab Z, Maliga P. The small, versatile pPZP family of *Agrobacterium* binary vectors for plant transformation. Plant Mol. Biol. 1994; 25:989–994. [PubMed: 7919218]

Harbour JW, Dean DC. Rb function in cell-cycle regulation and apoptosis. Nat. Cell Biol. 2000; 2:E65–E67. [PubMed: 10783254]

Hemerly A, Engler Jde A, Bergounioux C, van Montagu M, Engler G, Inze D, Ferreira P. Dominant negative mutants of the Cdc2 kinase uncouple cell division from iterative plant development. EMBO J. 1995; 14:3925–3936. [PubMed: 7664733]

Huntley R, Healy S, Freeman D, Lavender P, de Jager S, Greenwood J, Makker J, Walker E, Jackman M, Xie Q, et al. The maize retinoblastoma protein homologue ZmRb-1 is regulated during leaf development and displays conserved interactions with G1/S regulators and plant cyclin D (CycD) proteins. Plant Mol. Biol. 1998; 37:155–169. [PubMed: 9620273]

Joubes J, Chevalier C, Dudits D, Heberle-Bors E, Inze D, Umeda M, Renaudi JP. CDK-related protein kinases in plants. Plant Mol. Biol. 2000; 43:607–620. [PubMed: 11089864]

Kobor MS, Greenblatt J. Regulation of transcription elongation by phosphorylation. Biochim. Biophys. Acta. 2002; 1577:261–275. [PubMed: 12213657]

Laux T, Mayer KF, Berger J, Jurgens G. The *WUSCHEL* gene is required for shoot and floral meristem integrity in *Arabidopsis*. Development. 1996; 122:87–96. [PubMed: 8565856]

Lenhard M, Bohnert A, Jurgens G, Laux T. Termination of stem cell maintenance in *Arabidopsis* floral meristems by interactions between *WUSCHEL* and *AGAMOUS*. Cell. 2001; 105:805–814. [PubMed: 11440722]

Li J, Chen X. PAUSED, a putative exportin-t, acts pleiotropically in *Arabidopsis* development but is dispensable for viability. Plant Physiol. 2003; 132:1913–1924. [PubMed: 12913148]

Li J, Jia D, Chen X. *HUA1*, a regulator of stamen and carpel identities in *Arabidopsis*, codes for a nuclear RNA binding protein. Plant Cell. 2001; 13:2269–2281. [PubMed: 11595801]

Liao SM, Zhang J, Jeffery DA, Koleske AJ, Thompson CM, Chao DM, Viljoen M, van Vuuren HJ, Young RA. A kinase-cyclin pair in the RNA polymerase II holoenzyme. Nature. 1995; 374:193–196. [PubMed: 7877695]

Lohmann JU, Hong RL, Hobe M, Busch MA, Parcy F, Simon R, Weigel D. A molecular link between stem cell regulation and floral patterning in *Arabidopsis*. Cell. 2001; 105:793–803. [PubMed: 11440721]

Magyar Z, Meszaros T, Miskolczi P, Deak M, Feher A, Brown S, Kondorosi E, Athanasiadis A, Pongor S, Bilgin M, et al. Cell cycle phase specificity of putative cyclin-dependent kinase variants in synchronized alfalfa cells. Plant Cell. 1997; 9:223–235. [PubMed: 9061953]

Mandel MA, Gustafson-Brown C, Savidge B, Yanofsky MF. Molecular characterization of the *Arabidopsis* floral homeotic gene *APETALA1*. Nature. 1992; 360:273–277. [PubMed: 1359429]

Mariconti L, Pellegrini B, Cantoni R, Stevens R, Bergounioux C, Cella R, Albani D. The E2F family of transcription factors from *Arabidopsis thaliana* Novel and conserved components of the retinoblastoma/E2F pathway in plants. J. Biol. Chem. 2002; 277:9911–9919. [PubMed: 11786543]

Mayer KF, Schoof H, Haecker A, Lenhard M, Jurgens G, Laux T. Role of *WUSCHEL* in regulating stem cell fate in the *Arabidopsis* shoot meristem. Cell. 1998; 95:805–815. [PubMed: 9865698]

Meijer M, Murray JAH. The role and regulation of D-type cyclins in the plant cell cycle. Plant Mol. Biol. 2000; 43:621–633. [PubMed: 11089865]

Meyerowitz EM, Bowman JL, Brockman LL, Drews GN, Jack T, Sieburth LE, Weigel D. A genetic and molecular model for flower development in *Arabidopsis thaliana*. Development Suppl. 1991:157–167.

Morgan DO. Cyclin-dependent kinases: engines, clocks, and microprocessors. Annu. Rev. Cell Dev. Biol. 1997; 13:261–291. [PubMed: 9442875]

Nakagami H, Sekine M, Murakami H, Shinmyo A. Tobacco retinoblastoma-related protein phosphorylated by a distinct cyclin-dependent kinase complex with Cdc2/cyclin D in vitro. Plant J. 1999; 18:243–252. [PubMed: 10377991]

Nelson C, Goto S, Lund K, Hung W, Sadowski I. Srb10/Cdk8 regulates yeast filamentous growth by phosphorylating the transcription factor Ste12. Nature. 2003; 421:187–190. [PubMed: 12520306]

Oelgeschlager T. Regulation of RNA polymerase II activity by CTD phosphorylation and cell cycle control. J. Cell Physiol. 2002; 190:160–169. [PubMed: 11807820]

Park W, Li J, Song R, Messing J, Chen X. CARPEL FACTORY, a Dicer homolog, and HEN1, a novel protein, act in microRNA metabolism in *Arabidopsis thaliana*. Curr. Biol. 2002; 12:1484–1495. [PubMed: 12225663]

Pelaz S, Ditta GS, Baumann E, Wisman E, Yanofsky MF. B and C floral organ identity functions require *SEPALLATA* MADS-box genes. Nature. 2000; 405:200–203. [PubMed: 10821278]

Porceddu A, Stals H, Reichheld JP, Segers G, de Veylder L, Barroco RP, Casteels P, van Montagu M, Inze D, Mironov V. A plant-specific cyclin-dependent kinase is involved in the control of G2/M progression in plants. J. Biol. Chem. 2001; 276:36354–36360. [PubMed: 11477067]

Rickert P, Seghezzi W, Shanahan F, Cho H, Lees E. Cyclin C/CDK8 is a novel CTD kinase associated with RNA polymerase II. Oncogene. 1996; 12:2631–2640. [PubMed: 8700522]

Riou-Khamlichi C, Huntley R, Jacqmard A, Murray JA. Cytokinin activation of *Arabidopsis* cell division through a D-type cyclin. Science. 1999; 283:1541–1544. [PubMed: 10066178]

Schoof H, Lenhard M, Haecker A, Mayer KF, Jürgens G, Laux T. The stem cell population of *Arabidopsis* shoot meristems is maintained by a regulatory loop between the *CLAVATA* and *WUSCHEL* genes. Cell. 2000; 100:635–644. [PubMed: 10761929]

Sugimoto-Shirasu K, Roberts K. “Big it up”: endoreduplication and cell-size control in plants. Curr. Opin. Plant Biol. 2003; 6:544–553. [PubMed: 14611952]

Sun X, Zhang Y, Cho H, Rickert P, Lees E, Lane W, Reinberg D. NAT, a human complex containing Srb polypeptides that functions as a negative regulator of activated transcription. Mol. Cell. 1998; 2:213–222. [PubMed: 9734358]

Takeda K, Saito T, Ochiai H. A novel *Dictyostelium* Cdk8 is required for aggregation, but is dispensable for growth. Develop. Growth Differ. 2002; 44:213–223.

Ubersax JA, Woodbury EL, Quang PN, Paraz M, Blethrow JD, Shah K, Shokat KM, Morgan DO. Targets of the cyclin-dependent kinase Cdk1. Nature. 2003; 425:859–864. [PubMed: 14574415]

Vandepoele K, Raes J, de Veylder L, Rouze P, Rombauts S, Inze D. Genome-wide analysis of core cell cycle genes in *Arabidopsis*. Plant Cell. 2002; 14:903–916. [PubMed: 11971144]

Wasteneys GO, Galway ME. Remodeling the cytoskeleton for growth and form: an overview with some new views. Annu. Rev. Plant Biol. 2003; 54:691–722. [PubMed: 14503008]

Western TL, Cheng Y, Jun L, Chen X. HUA ENHANCER2, a putative DExH-box RNA helicase, maintains homeotic B and C gene expression in *Arabidopsis*. Development. 2002; 129:1569–1581. [PubMed: 11923195]

Xie Q, Sanz-Burgos AP, Hannon GJ, Gutierrez C. Plant cells contain a novel member of the retinoblastoma family of growth regulatory proteins. EMBO J. 1996; 15:4900–4908. [PubMed: 8890163]

Yamaguchi M, Fabian T, Sauter M, Bhalerao RP, Schrader J, Sandberg G, Umeda M, Uchimiya H. Activation of CDK-activating kinase is dependent on interaction with H-type cyclins in plants. Plant J. 2000; 24:11–20. [PubMed: 11029700]

Yanofsky MF, Ma H, Bowman JL, Drews GN, Feldmann KA, Meyerowitz EM. The protein encoded by the *Arabidopsis* homeotic gene *AGAMOUS* resembles transcription factors. Nature. 1990; 346:35–39. [PubMed: 1973265]

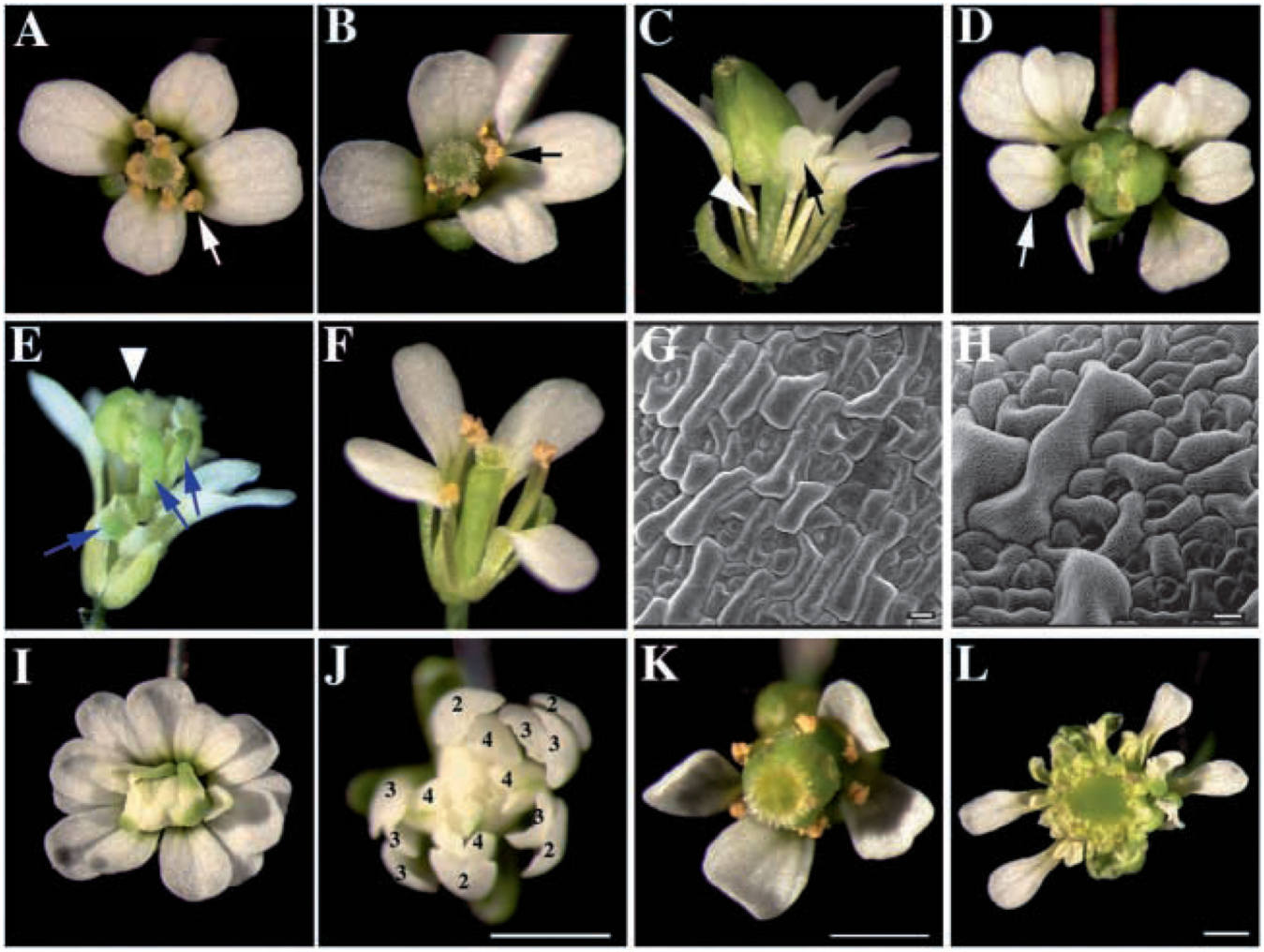

Fig. 1.

Floral phenotypes caused by *hen3* mutations. (A) A wild-type flower with stamens in the third whorl (arrow) and carpels in the fourth whorl. (B) A *hua1-1 hua2-1* flower with stamens in the third whorl (arrow) and carpels in the fourth whorl. (C) A *hua1-1 hua2-1 hen3-1* flower with petals in the third whorl (arrow) and an enlarged gynoecium with a gynophore at the base (arrowhead), which indicates that the gynoecium has partial floral character. (D) A *hua1-1 hua2-1 hen3-2* flower with petals in the third whorl (arrow) and an enlarged gynoecium in the center. (E) A *hua1-1 hua2-1 hen3-3* flower with an additional flower in the center (arrowhead). The blue arrows indicate three unfused carpels. (F) A *hen3-1* flower with normal organ identity. (G) Epidermal valve cells with a smooth surface from the bottom of a *hua1-1 hua2-1* ovary. (H) Epidermal valve cells from a *hua1-1 hua2-1 hen3-1* ovary. The cells have epicuticular striations similar to epidermal cells on sepals. (I) A *hua1-1 hua2-1 hen3-1 ag-1* flower. (J) A *hen3-1 ag-1* flower. The numbers indicate the floral whorls. The fourth whorl sepals are largely transformed to petals. (K) A *clv1-4* flower. (L) A *hua1-1 hua2-1 hen3-1 clv1-4* flower, with a massive amount of undifferentiated cells in the center. Scale bars: 10 μm in G,H; 1 mm in J–L.

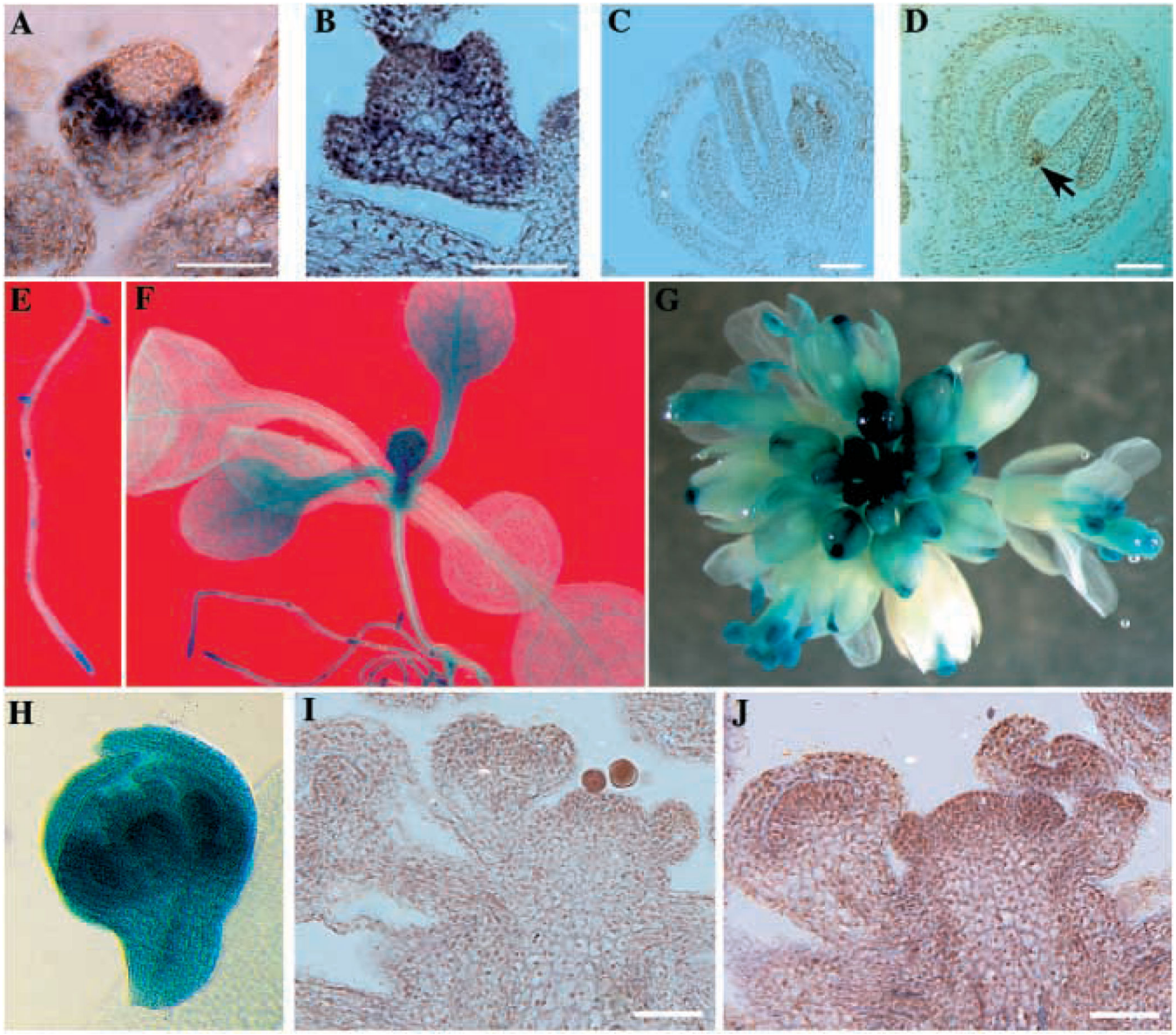

Fig. 2.

Expression patterns of *AP1, WUS*, and *HEN3* in plants. (A,B) In situ hybridization on sections of stage 3 flowers to detect *AP1* RNA. (A) A *hua1-1 hua2-1* flower. (B) A *hua1-1 hua2-1 hen3-1* flower. *AP1* RNA is found throughout the flower in *hua1-1 hua2-1 hen3-1*. (C,D) In situ hybridization on sections of stage 9 flowers to detect *WUS* RNA. (C) A stage 9 *hua1-1 hua2-1* flower that has ceased to express *WUS*. (D) A stage 9 *hua1-1 hua2-1 hen3-1* flower that still expresses *WUS* (arrow). (E–H) GUS staining of HEN3-GUS transgenic lines. HEN3-GUS is found in proliferating tissues or organs. (E) HEN3-GUS is present at the root tip and lateral root primordia. (F) HEN3-GUS is present at the shoot tip, in young leaves, and at the base of growing leaves. (G) HEN3-GUS is present in young flowers. (H) HEN3-GUS is found throughout a stage 7 flower. (I,J) In situ hybridization on longitudinal sections of wild-type inflorescences using either the sense (I) or the antisense (J) *HEN3*

probe. *HEN3* RNA is found at a low level throughout the inflorescence meristem and the floral meristems. Scale bars: 50 μm.

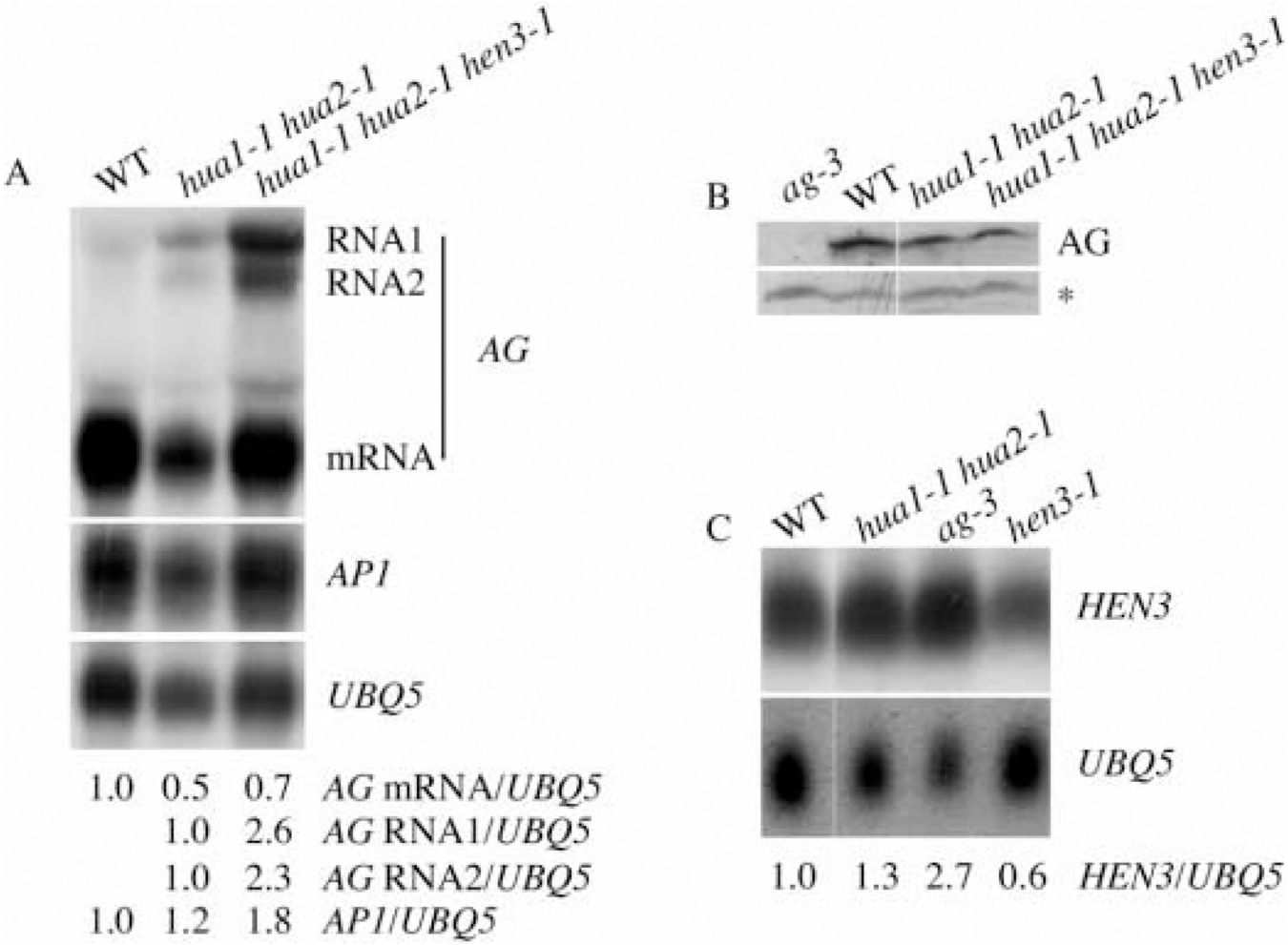

Fig. 3.

AP1, AG and *HEN3* expression in various genotypes. (A) RNA filter hybridization to examine *AG* and *AP1* RNA levels in various genotypes as indicated. The two *AG* RNAs containing 2nd intron sequences are marked as RNA1 and RNA2. The abundance of *AP1* and *AG* RNAs is indicated by the numbers below the gel images. (B) Western blotting on total proteins from inflorescences from various genotypes using anti-AG antisera. *ag-3* serves as a negative control. AG protein abundance is similar in *hua1-1 hua2-1* and *hua1-1 hua2-1 hen3-1* flowers. The band marked by an asterisk is a crossreacting, non-AG species from the same blot. (C) RNA filter hybridization to determine the abundance of *HEN3* RNA from inflorescences of various genotypes. The abundance relative to wild type is indicated by numbers below the gel images.

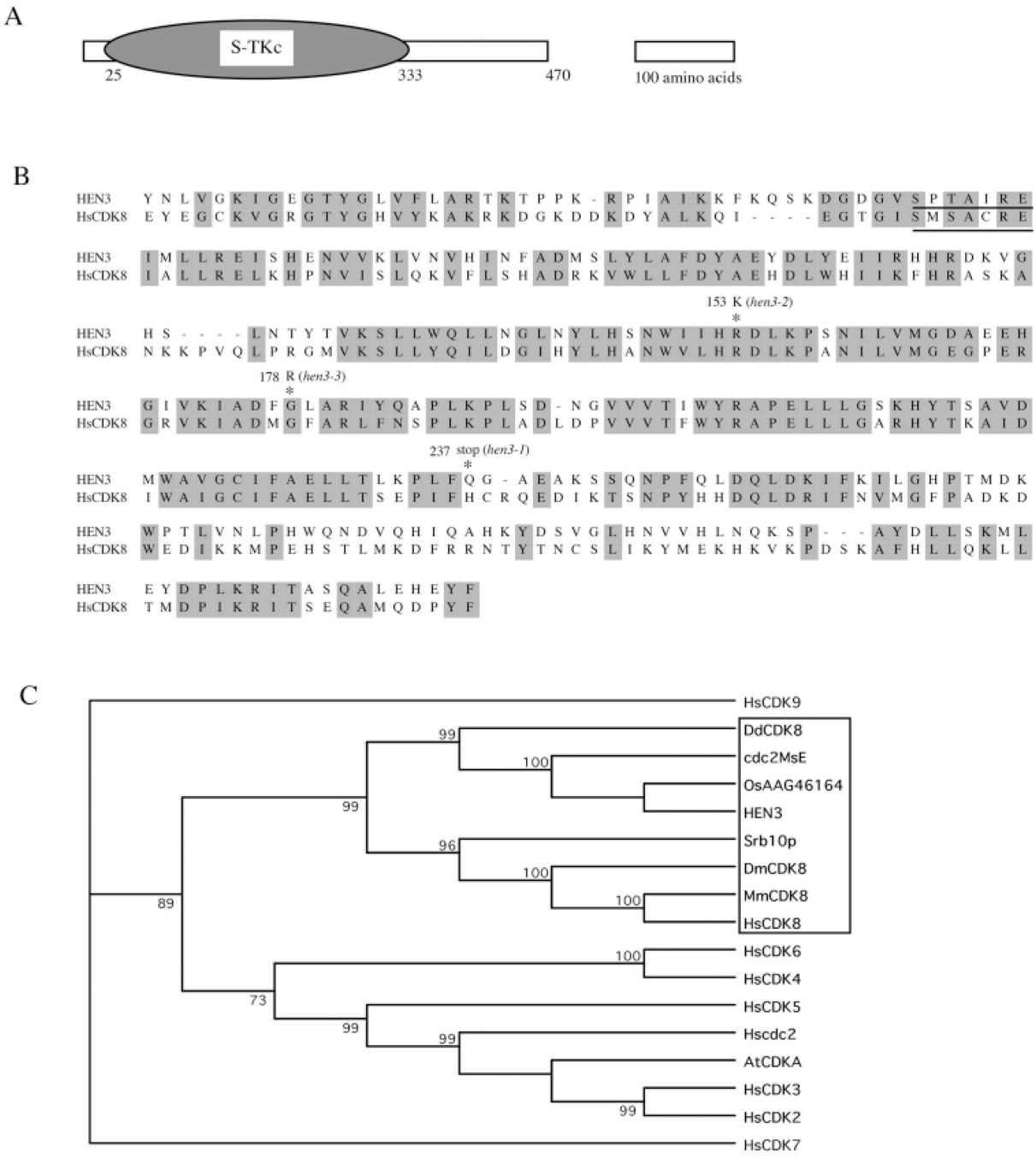

Fig. 4.

HEN3 is closely related to CDK8. (A) A diagram of HEN3 protein with the serine-threonine kinase domain represented by the oval. (B) A Clustal W alignment of the kinase domains in HEN3 and human CDK8. Identical and similar amino acids are shaded. The amino acid positions and nature of the three *hen3* alleles are indicated above the sequences. The cyclin-binding motifs of HEN3 and CDK8 are underlined. (C) A bootstrap consensus phylogenetic tree involving nine different human CDKs, CDK8 from *Drosophila* (DmCDK8), mouse (MmCDK8), *Dictyostelium* (DdCDK8) and yeast (Srb10p), three E type CDKs from plants,

and the *Arabidopsis* CDKA (AtCDKA). Cdc2MsE and OsAAG46164 are CDKEs from alfalfa and rice, respectively. The tree was constructed using the neighbor joining method and the bootstrap consensus was generated from 1000 replications. The numbers represent the percentage occurrence of the nodes in the replications. Only the protein kinase domains from these proteins were used in the analysis. The CDK8 clade is indicated by the rectangle.

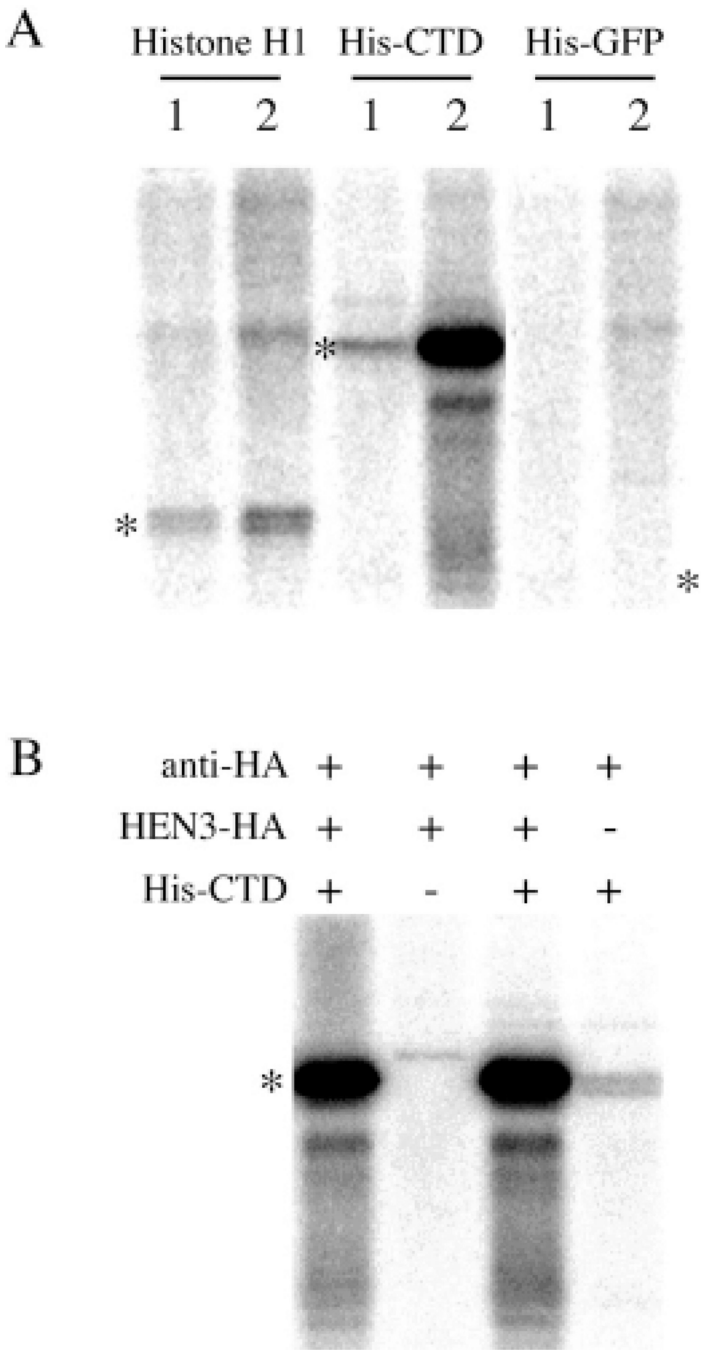

Fig. 5.

HEN3 has CTD kinase activity. HEN3-HA transgenic plants or control non-transgenic plants were immunoprecipitated with an anti-HA monoclonal antibody, and the immunoprecipitate was used in a kinase assay with 10 μg purified histone H1, 6×His-CTD or 6×His-GFP as substrates. The positions of the substrate proteins are illustrated by the asterisks. The amount of substrate proteins is identical in each lane. (A) The anti-HA (lanes 2) but not the anti-protein C (lanes 1) immunoprecipitate from HEN3-HA transgenic plants displays kinase activity on 6×His-CTD. Histone H1 and 6×His-GFP are not phosphorylated by the anti-HA

immunoprecipitate. (B) The anti-HA immunoprecipitate from HEN3-HA transgenic plants but not from wild-type plants phosphorylates 6×His-CTD.

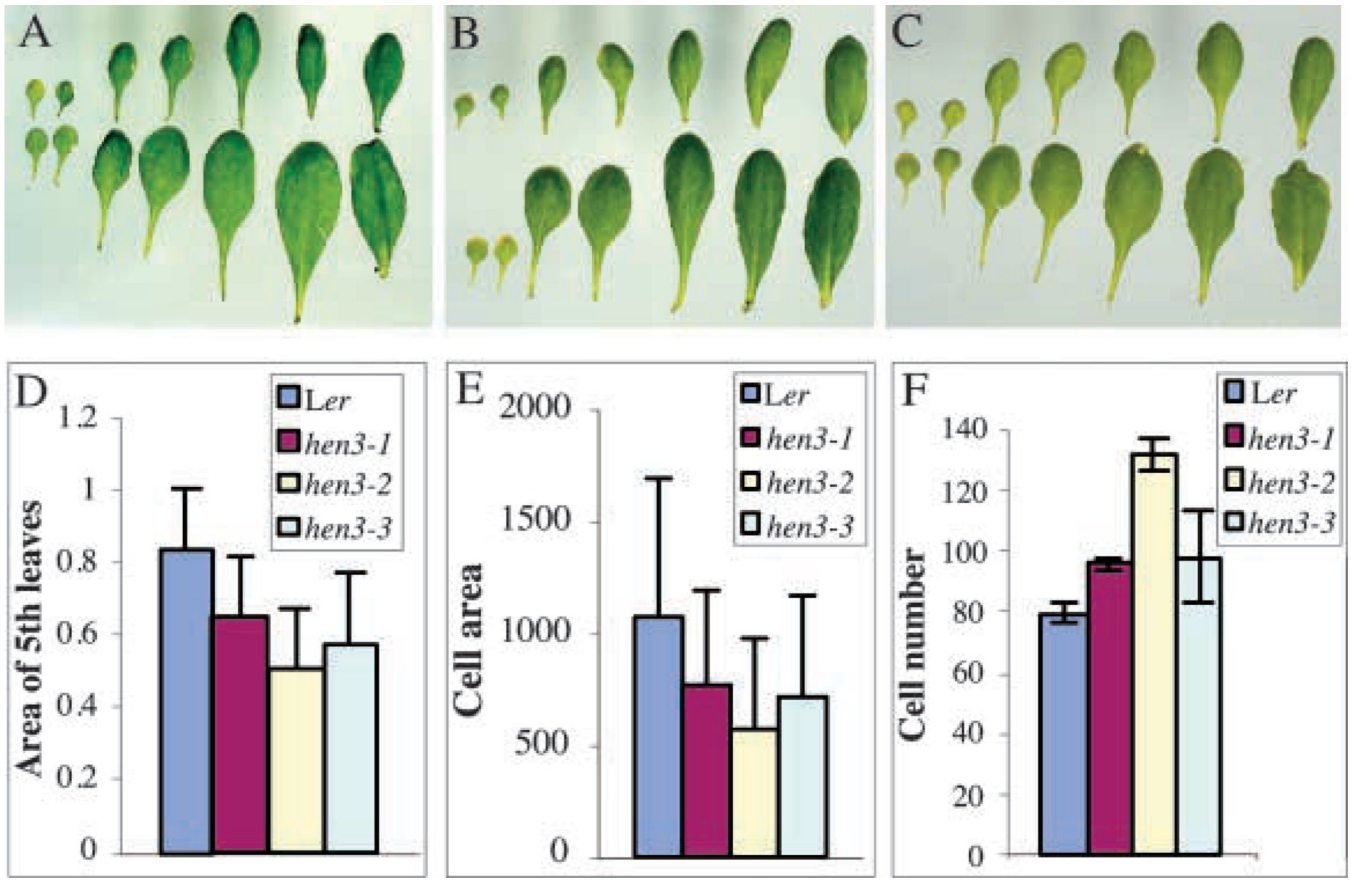

Fig. 6.

Effects of *hen3* mutations on leaf size and leaf epidermal cell size. (A–C) Dissected rosette leaves 1–7 (arranged from left to right) from *hen3* (top) and wild-type (bottom) plants that were grown side by side. (A) *hen3-1* and wild type. (B) *hen3-2* and wild type. (C) *hen3-3* and wild type. Note that the first two leaves are not affected as much as the later leaves by the *hen3* mutations. The *hen3* mutations all lead to a reduction in leaf size. (D) Area (cm^2) of the fully expanded fifth leaf from wild-type and *hen3* genotypes. Ten leaves were measured for each genotype. (E) Surface area (μm^2) of adaxial epidermal cells on the fifth leaf of wild-type and *hen3* genotypes. The number of cells measured was 95, 141, 173 and 143 for wild type, *hen3-1, hen3-2* and *hen3-3*, respectively. The large standard error is largely due to the intrinsic variation in cell size on the leaf epidermis. (F) Number of epidermal pavement cells in a 70,000 μm^2 area from similar positions in the fifth leaves of various genotypes. Measurements were performed on SEM images of three leaves from each genotype. The error bars in D–F represent standard errors.

Table 1

Floral organ count in *hua1-1 hua2-1, hua1-1 hua2-1 hen3-1*, and *hua1-1 hua2-1 hen3-2*

	Whorl 3					Whorl 4		
	Stamen	**Petaloid stamen**	**Filament**	**Petal**	**Total**	**Carpel***	**Sepal***	**Total**
hua1-1 hua2-1 (*n*=100)	4.9±0.7	0.1±0.4			5.1±0.7	2.0±0.0		2.0±0.0
hua1-1 hua2-1 hen3-1 (*n*=100)		0.1±0.5	0.1±0.2	5.3±0.8	5.5±0.6	2.4±1.1	0.9±1.2	3.2±0.7
hua1-1 hua2-1 hen3-2 (*n*=48)			1.5±1.3	3.7±1.5	5.2±0.7	2.3±1.1	0.8±1.2	3.2±0.7

*Organs with stigmatic tissue were counted as carpels while those without stigmatic tissue were considered sepals.

n, the number of flowers counted.

The number and identity of the outer two whorls of organs were normal in the three genotypes and are not shown.